Transverse Ising chain under periodic instantaneous quenches: Dynamical many-body freezing and emergence of slow solitary oscillations

Sirshendu Bhattacharyya
R.R.R. Mahavidyalaya, Radhanagar, Hooghly, India

Arnab Das*
Theoretical Division (T-4), LANL, MS-B213, Los Alamos, New Mexico 87545, USA and Max-Planck Institute for the Physics of Complex Systems, Nöthnitzer Strasse 38, Dresden 01187, Germany

Subinay Dasgupta
Department of Physics, University of Calcutta, 92 Acharya Prafulla Chandra Road, Kolkata 700009, India
(Received 17 January 2012; revised manuscript received 29 May 2012; published 8 August 2012)

We study the real-time dynamics of a quantum Ising chain driven periodically by instantaneous quenches of the transverse field between $+\Gamma_0$ and Γ_0 back and forth in equal intervals of time. Two interesting phenomena are reported and analyzed. (i) We observe dynamical many-body freezing (DMF), i.e., strongly nonmonotonic freezing of the response with respect to the driving parameters (pulse width and height) resulting from coherent suppression of dynamics of *all* quasiparticle modes. For certain combinations of the pulse height and the period, maximal freezing (DMF peaks) is observed, where a massive collapse of the entire Floquet spectrum occurs and the many-body system remains frozen extremely close to the initial state for all time. (ii) Second, away from the freezing peak, we observe the emergence of a distinct oscillation with a single nontrivial frequency, which can be much lower than the driving frequency. This remarkable slow oscillation involving many high-energy modes dominates the response in the limit of long observation time. We identify this slow oscillation as the unique survivor of destructive quantum interference between the many-body modes. The oscillation tends to decay algebraically with time to a constant value. All the key features are demonstrated analytically with numerical evaluations for specific results.

DOI: 10.1103/PhysRevB.86.054410 PACS number(s): 03.65.−w, 75.45.+j, 37.10.Ty, 05.30.−d

I. INTRODUCTION

Nonequilibrium dynamics of driven quantum many-body systems is an emerging paradigm for studying and unveiling new quantum phenomena. The last few years have witnessed a surge of theoretical endeavors in understanding the dynamics of quantum many-body systems under simple drivings. A major part of these recent activities is concentrated around quantum quenches, leading to several interesting and novel issues including (but not limited to) universal quench dynamics across quantum critical points—the associated quantum Kibble-Zurek mechanism, the physics of nonequilibrium excitations, and the physics of thermalization in quantum systems (see for a review, Ref. 1; and C. de Grandi *et al*., S. Mondal *et al*., and U. Divkaran *et al*., in Ref. 2 and references therein). The main focuses of these studies, namely, the final defect density following a quantum quench, or the effective temperature in a thermalized system, however, are insensitive to the details of the quantum coherence of the underlying many-body dynamics. For example, the dynamical idea behind the quantum Kibble-Zurek mechanism[3] is a robust translation of the classical Kibble-Zurek idea[4] to quantum systems—of course, the origins of the relevant length scales and time scales are different.

Here we focus on another important class of driven quantum nonequilibrium phenomena, where quantum coherence plays the central role. Though nonadiabaticity is a common covering for all interesting nonequilibrium phenomena, here *coherent* quantum mechanical suppression of dynamics contributes crucially to the nonadiabaticity of the dynamics which makes the resulting response behavior difficult to explain using classical intuitions. We discuss the dynamics of periodically driven quantum many-body systems. Coherent periodic driving can give rise to surprising phenomena in quantum many-body systems, which counters our classical intuitions drastically.[5] The role of quantum coherence in the important context of a superfluid-insulator transition realized in a periodically driven optical lattice has been demonstrated earlier.[6,7] Owing to the experimental breakthrough in attaining long coherence time in quantum many-body systems in the last decade, for example, within the framework of atoms/ions in optical lattices and traps, this coherent regime is becoming more and more accessible experimentally (see, e.g., Refs. 8–12). Here we study the coherent dynamics (Schrödinger dynamics at zero temperature) of a simple paradigmatic system—the transverse Ising chain[13] subjected to a train of rectangular pulses of the transverse field. Two interesting phenomena are reported—both of which are purely quantum mechanical in origin and are the result of coherent many-body dynamics.

It has been observed recently that a class of integrable quantum many-body systems exhibits the phenomena of dynamical many-body freezing (DMF), i.e. nonmonotonic freezing behavior of *all* the many-body modes when driven externally by varying a parameter in the Hamiltonian continuously,[5] The said freezing behavior is counterintuitive to the "classical" picture of a driven system falling out of equilibrium. The classical behavior arises from competition of two time scales: the driving period and the characteristic relaxation time of the system (see, however, Ref. 14). Contrary to the expected monotonically increasing freezing behavior of the system with respect to the driving frequency according to that picture, we observe strongly nonmonotonic freezing behavior, with maximal freezing for certain combinations of driving amplitude and frequency. A related phenomena, observed in the context of a single particle localized in a periodically driven potential—known as dynamical localization or, synonymously, coherent destruction of tunneling (CDT), is well studied.[15–19] In Ref. 19, interestingly, it has been shown in the context of periodically driven BEC, that the driving can lead to steady BEC-like states which are different from the equilibrium ground state of the undriven Hamiltonian. The above findings motivate us to investigate such phenomena in a pulse driven many-body system, where, instead of a smoothly varying driving rate, we have sequences of instantaneous quenches and subsequent waiting times. Here we observe DMF, confirming the generality of the phenomena beyond sinusoidal driving. We deduce the exact condition for the maximal freezing analytically and explore other characteristics of the freezing phenomena.

In addition to DMF, we observe another interesting phenomena away from the freezing peaks. In the limit of long observation time, we see spectacular dominance of a single long-lived oscillation (with frequency much smaller than the driving frequency) in the response dynamics. Surprisingly, this happens even in the limit of strong and fast driving (pulse amplitude and frequency much larger than the interspin coupling). We discuss the origin and nature of this intriguing quantum oscillation.

II. THE MODEL AND THE DYNAMICS

We quench the transverse field Γ from $+\Gamma_0$ to $-\Gamma_0$ and back in successive time intervals of duration T in a transverse Ising chain Hamiltonian:

$$\mathcal{H} = -J\sum_{j=1}^{N} s_j^x s_{j+1}^x - \Gamma(t)\sum_{j=1}^{N} s_j^z, \tag{1}$$

where the field $\Gamma(t)$ varies like a square wave with period T at $t = 0$:

$$\Gamma(t) = \begin{cases} \Gamma_0 & \text{for} \quad nT < t < (n+\frac{1}{2})T, \\ -\Gamma_0 & \text{for} \quad (n+\frac{1}{2})T < t < (n+1)T, \end{cases} \tag{2}$$

with $n = 0,1,2,\ldots$ and $\Gamma_0 > 0$. We set the energy scale by taking $J = 1$. In order to investigate the dynamics in this case, first we diagonalize Hamiltonian (1) for a given value of Γ by the Jordan-Wigner transformation followed by Fourier transform.[20] This transforms the Hamiltonian (1) into a direct sum of Hamiltonians of nonlocal free fermions of momenta k. The Hamiltonian preserves the parity of the fermion number (even/odd) and the ground state always lies in the even-fermionic sector. We work with the projection of the Hamiltonian in this sector, given by

$$\begin{aligned} \mathcal{H} &= \bigoplus_{k>0} \mathcal{H}_k, \\ \mathcal{H}_k &= (-2i\sin k)[a_k^\dagger a_{-k}^\dagger + a_k a_{-k}] \\ &\quad - 2(\Gamma + \cos k)[a_k^\dagger a_k + a_{-k}^\dagger a_{-k} - 1], \end{aligned} \tag{3}$$

where $k = (2n+1)\pi/N$, $n = 0,1,\ldots,N/2-1$. The ground state of $\mathcal{H}_k$ is a linear combination of the fermionic occupation number basis states $|0\rangle_k = |0_k,0_{-k}\rangle$ (both $\pm k$ levels unoccupied) and $|1\rangle_k = |1_k,1_{-k}\rangle$ (both $\pm k$ levels occupied), and the Hamiltonian does not couple them with the two other basis states $|0_k,1_{-k}\rangle$ and $|1_k,0_{-k}\rangle$. Hence starting with the ground state, the dynamics always remains confined within a manifold which is the direct product of the two-dimensional subspaces spanned by $|0\rangle_k$ and $|1\rangle_k$. We denote the eigenstates of $\mathcal{H}_k$ within these subspaces as $|(\Gamma,k)_-\rangle$ (ground state) and $|(\Gamma,k)_+\rangle$, with eigenvalues $-\lambda(\Gamma,k)$ and $\lambda(\Gamma,k)$, where

$$\lambda(\Gamma,k) = 2\sqrt{\Gamma^2 + 1 + 2\Gamma\cos k}, \tag{4}$$

$$|(\Gamma,k)_-\rangle = i\cos\theta|1\rangle_k - \sin\theta|0\rangle_k, \tag{5}$$

$$|(\Gamma,k)_+\rangle = i\sin\theta|1\rangle_k + \cos\theta|0\rangle_k, \tag{6}$$

$$\tan\theta = \frac{-\sin k}{\Gamma + \cos k + \sqrt{\Gamma^2 + 1 + 2\Gamma\cos k}}. \tag{7}$$

We now solve the Schrödinger equation

$$i\hbar\frac{\partial|\psi_k\rangle}{\partial t} = \mathcal{H}_k|\psi_k\rangle, \tag{8}$$

where the wave function in the time-dependent energy eigenbasis may be expressed as

$$|\psi_k\rangle = x_-(t)|(\Gamma,k)_-(t)\rangle + x_+(t)|(\Gamma,k)_+(t)\rangle. \tag{9}$$

If $\Gamma(t)$ is constant (say, Γ_0) over a time interval t_0 to t, then we have

$$x_\pm(t) = x_\pm(t_0)\exp\left\{\mp\frac{i}{\hbar}(t-t_0)\lambda(\Gamma_0,k)\right\}. \tag{10}$$

At time $t = 0$ let the system be in the state

$$|\psi_k\rangle = \alpha|(\Gamma_0,k)_-\rangle + \beta|(\Gamma_0,k)_+\rangle, \tag{11}$$

with $|\alpha|^2 + |\beta|^2 = 1$. Then according to Eq. (10) at $t = \frac{T}{2} - \epsilon$ (where ϵ is a small positive number), the coefficients are given by

$$\begin{pmatrix} x_-(\frac{T}{2}-\epsilon) \\ x_+(\frac{T}{2}-\epsilon) \end{pmatrix} = \begin{pmatrix} e^{i\mu_1} & 0 \\ 0 & e^{-i\mu_1} \end{pmatrix}\begin{pmatrix} \alpha \\ \beta \end{pmatrix}, \tag{12}$$

where

$$\mu_1 = \frac{T}{2\hbar}\lambda(\Gamma_0,k). \tag{13}$$

Using the continuity of $|\psi_k\rangle$ at $t = \frac{T}{2}$ one obtains the wave function at $t = \frac{T}{2} + \epsilon$ in terms of $|(-\Gamma_0,k)_-\rangle$ and $|(-\Gamma_0,k)_+\rangle$. Time evolution in the second half proceeds in the same way as in the first half and the transformation over one full cycle is given by

$$\begin{pmatrix} x_-(T+\epsilon) \\ x_+(T+\epsilon) \end{pmatrix} = \mathbf{U}_k\begin{pmatrix} \alpha \\ \beta \end{pmatrix}, \tag{14}$$

where

$$\begin{aligned} \mathbf{U}_k &= \begin{pmatrix} \cos\phi & -\sin\phi \\ \sin\phi & \cos\phi \end{pmatrix}\begin{pmatrix} e^{i\mu_2} & 0 \\ 0 & e^{-i\mu_2} \end{pmatrix} \\ &\quad \times \begin{pmatrix} \cos\phi & \sin\phi \\ -\sin\phi & \cos\phi \end{pmatrix}\begin{pmatrix} e^{i\mu_1} & 0 \\ 0 & e^{-i\mu_1} \end{pmatrix}. \end{aligned} \tag{15}$$

Here

$$\mu_2 = \frac{T}{2\hbar}\lambda(-\Gamma_0,k) \quad \text{and} \quad \phi = \theta_1 - \theta_2, \tag{16}$$

where θ_1 and θ_2 are the values of θ [as defined in Eq. (7)] for $\Gamma = +\Gamma_0$ and $-\Gamma_0$, respectively.

During the first half-cycle after n full cycles, at a time $t = nT + \tau$ with $0 < \tau < \frac{T}{2}$, the coefficients are given by

$$\begin{pmatrix} x_-(nT+\tau) \\ x_+(nT+\tau) \end{pmatrix} = \begin{pmatrix} e^{i\mu_3} & 0 \\ 0 & e^{-i\mu_3} \end{pmatrix} \mathbf{U}_k^n \begin{pmatrix} \alpha \\ \beta \end{pmatrix}, \tag{17}$$

where $\mu_3 = \frac{\tau}{\hbar}\lambda(\Gamma_0,k)$. Similarly, during the second half-cycle after n full cycles, at a time $t = nT + \frac{T}{2} + \tau$, the coefficients are given by

$$\begin{pmatrix} x_-(nT+\frac{T}{2}+\tau) \\ x_+(nT+\frac{T}{2}+\tau) \end{pmatrix} = \begin{pmatrix} e^{i\mu_4} & 0 \\ 0 & e^{-i\mu_4} \end{pmatrix} \begin{pmatrix} \cos\phi & \sin\phi \\ -\sin\phi & \cos\phi \end{pmatrix} \times \begin{pmatrix} e^{i\mu_1} & 0 \\ 0 & e^{-i\mu_1} \end{pmatrix} \mathbf{U}_k^n \begin{pmatrix} \alpha \\ \beta \end{pmatrix}, \tag{18}$$

where $\mu_4 = \frac{\tau}{\hbar}\lambda(-\Gamma_0,k)$.

Transverse magnetization M_z (per spin) at any time is given by

$$M_z = -1 + \frac{4}{N}\sum_{k=0}^{\pi} M_k = -1 + \frac{2}{\pi}\int_0^{\pi} M_k dk, \tag{19}$$

where $M_k = \frac{1}{2}\langle\psi_k|(a_k^* a_k + a_{-k}^* a_{-k})|\psi_k\rangle$. From Eqs. (5) and (6),

$$M_k = |(x_- \cos\theta_j + x_+ \sin\theta_j)|^2, \tag{20}$$

with $j = 1$ or 2 according to whether we are in the first or second half-cycle, respectively.

In order to calculate $\mathbf{U}_k^n$, giving the time evolution after the nth cycle, we note that, for any 2×2 matrix,

$$\mathbf{U}_k^2 = -(\mathrm{Tr}\,\mathbf{U}_k)\mathbf{1} + (\det \mathbf{U}_k)\mathbf{U}_k.$$

This shows that one can write

$$\mathbf{U}_k^n = a_n\mathbf{1} + b_n\mathbf{U}_k. \tag{21}$$

The recursion relations for a_n and b_n can be easily solved to get

$$a_n = -b_{n-1} \quad \text{and} \quad b_n = \sin(n\omega_k)/\sin\omega_k. \tag{22}$$

where $\cos\omega_k = \cos(\mu_1+\mu_2)\cos^2\phi + \cos(\mu_1-\mu_2)\sin^2\phi$. The expressions b_n are the Chebyshev polynomials of the second kind in $\cos\omega_k$.

III. DYNAMICAL MANY-BODY FREEZING

The system is initially ($t = 0$) in the ground state of the Hamiltonian with $\Gamma = +\Gamma_0$, before it is driven by the pulses. We have computed the magnetization numerically at any time (within a cycle) by obtaining x_- and x_+ from Eqs. (17) and (19), substituting them in Eq. (20) to get M_k, and then integrating it using Eq. (19). The result is presented in Fig. 1. Frames (a) and (b) show that the response, i.e., the transverse magnetization M_z, remains localized somewhere close to its initial value for all time. In other words, the response retains the memory of the breaking of the $\mathcal{Z}_2$ symmetry in the transverse direction by the polarized initial state through all later time, though the symmetry is respected by the driving over each complete cycle. The degree of symmetry breaking is given by the long-time average of M_z:

$$Q = \lim_{T_f\to\infty}\frac{1}{T_f}\int_0^{T_f} M_z(t)dt. \tag{23}$$

Q is also a measure of nonadiabatic freezing—if a driving were adiabatic, the resulting response would always follow the field (i.e., trace the instantaneous ground state value of the response) and thus would preserve the symmetry of the Hamiltonian over a period. The maximum amplitude of oscillation of M_z also determines the degree of freezing.

It is clear from Fig. 1 that for a given value of Γ_0, the nonadiabatic freezing Q is a strongly nonmonotonic function of T. When the condition

$$\frac{\Gamma_0 T}{\hbar} = \pi, 2\pi, 3\pi, \ldots \tag{24}$$

is satisfied the freezing attains a maximum (Q shows a peak), as shown in Figs. 1(b) and 1(c). Naively speaking, for a given Γ_0, if T is made larger, there is more time for the system to react to the successive flips made, and hence the response is expected to be more adiabatic (smaller Q and bigger response amplitude). This classical intuition clearly does not hold in this case, as the freezing (Q and response amplitude) is strongly nonmonotonic in T for a given Γ_0 [Fig. 1(a)]. Strong maximal freezing of the entire many-body system (Q peaks) observed for isolated points in the parameter space is also a surprising nonclassical feature of DMF, arising from coherent quantum dynamics.[5]

In order to derive the extremal freezing condition (24), we set $\tau = 0$ and evaluate $M_k(t = nT)$ as a function of n. Thus, we are basically looking at the start of every oscillation. Also, we assume that initially (at $t = 0$) the system was in the ground state for the transverse field at that moment. Thus, we set $\alpha = 1$ and $\beta = 0$ in Eq. (17), use Eq. (21) there, and obtain $x_-(nT)$ and $x_+(nT)$which are then substituted in Eq. (20). The result is

$$M_k = A_k + R_k\cos(2n\omega_k + \delta_k), \tag{25}$$

where

$$\begin{aligned} A_k &= \cos^2\theta_1 + g_k f_k, \\ R_k^2 &= g_k^2\left[f_k^2 + \sin^2(2\theta_1)\sin^2\mu_1\sin^2\omega_k\right], \\ \tan\delta_k &= \frac{1}{f_k}\sin(2\theta_1)\sin\mu_1\sin\omega_k, \end{aligned} \tag{26}$$

with

$$\begin{aligned} f_k &= \sin(2\theta_1)\sin\mu_1\cos\omega_k + \sin(2\theta_2)\sin\mu_2, \\ g_k &= \sin(2\phi)\sin(\mu_2)/(2\sin^2\omega_k) = |U_{12}|/(2\sin^2\omega_k), \end{aligned} \tag{27}$$

and

$$\omega_k = \cos^{-1}[\cos(\mu_1+\mu_2)\cos^2\phi + \cos(\mu_1-\mu_2)\sin^2\phi]. \tag{28}$$

From Eqs. (20) and (25) we see, the nonadiabatic freezing parameter Q [Eq. (23)] is given by

$$Q = -1 + \frac{2}{\pi}\int_0^{\pi} A_k dk. \tag{29}$$

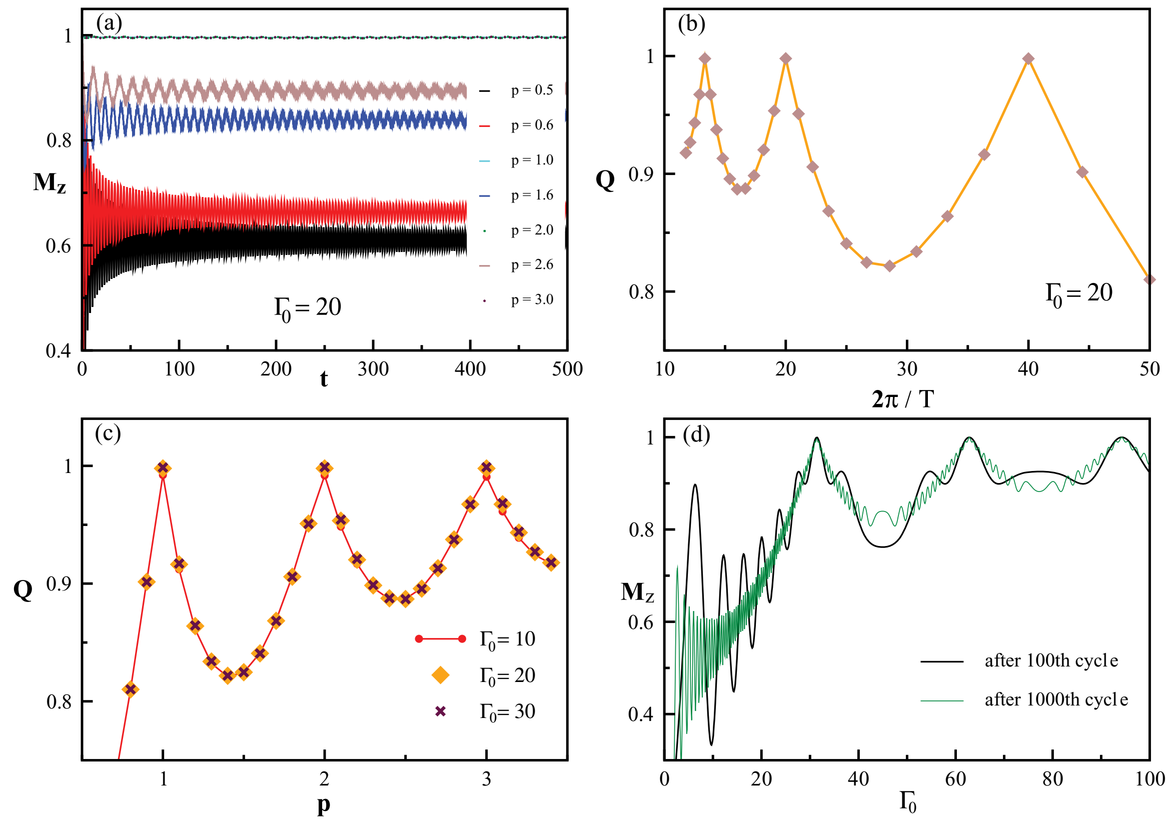

FIG. 1. (Color online) The DMF behavior of the resulting response. (a) Variation of M_z with t for different $p(p = \frac{\Gamma_0 T}{\pi})$ for $\Gamma_0 = 20$. (b) Variation of Q with $2\pi/T$ for $\Gamma_0 = 20$. (c) Variation of Q with p for different Γ_0. Maximal freezing is seen for integer p. (d) Magnetization after the 100th and the 1000th cycle at different Γ_0 for $T = 0.1$ ($\hbar = 1$).

Now, for large Γ_0, from Eqs. (13) and (16) we get

$$\phi = -\frac{\pi}{2} + \frac{\sin k}{\Gamma_0} + O\left(\frac{1}{\Gamma_0^3}\right), \quad \text{and}$$
$$\mu_2 = \frac{\Gamma_0 T}{\hbar}\left[1 - \frac{\cos k}{\Gamma_0} + O\left(\frac{1}{\Gamma_0^2}\right)\right]. \tag{30}$$

The off-diagonal elements of the transfer matrix $\mathbf{U}_k$ become then

$$U_{12} = i e^{-i\mu_1} \sin \mu_2 \sin 2\phi$$
$$= -i e^{-i\mu_1}\left[\sin\left(\frac{\Gamma_0 T}{\hbar}\right)\frac{2\sin k}{\Gamma_0} + O(1/\Gamma_0^2)\right] = -U_{21}^*. \tag{31}$$

Hence, according to Eq. (16) if $\frac{\Gamma_0 T}{\hbar}$ is an integral multiple of π, $\mathbf{U}_k$ becomes an identity matrix up to terms $1/\Gamma_0$ (since $\mu_1 \approx -\Gamma_0 T/\hbar$ for $\Gamma_0 \gg 1$), and the system is found at the initial state (approximately) after each cycle. Note that the freezing occurs for *any initial state*, irrespective of whether it is an eigenstate of the initial Hamiltonian or not. It is also consistent with the Floquet picture of quasienergy degeneracy (see, e.g., Refs. 21 and 22) employed in explaining dynamical localization. According to the Floquet theory, the above time evolution operator $\mathbf{U}_k$, which induces evolution from $t = 0$ to $t = T$, should have the general form $\mathbf{U}_k = e^{i\mathbf{M_k}t}$, where $\mathbf{M_k}$ is a time-independent Hermitian matrix (sharing the same dimension and space as $\mathbf{U}_k$),[21] with eigenvectors denoted by $|\mu_{1k}\rangle$ and $|\mu_{2k}\rangle$ corresponding to eigenvalues μ_{1k} and μ_{2k}, which are the Floquet quasienergies. Now as we have shown, in our case $\mathbf{U}_k$ tends to the Identity matrix up to term $1/\Gamma_0$ in large Γ_0 limit, which means both its eigenvalues $e^{i\mu_{1k}}$ and $e^{i\mu_{1k}}$ tend to unity for every k within the said approximation, resulting in a massive quasienergetic degeneracy all over the many-body spectrum—the crux of DMF. Recently, another interesting manifestation of DMF is observed in periodically driven bosons in optical lattice with low frequency sinusoidal driving across the tip of the Mott lobe.[23]

The mechanism of strong DMF with rectangular driving can be visualized by appealing to the simplicity of the driving—it consists of dynamics driven by two piecewise time-independent Hamiltonians $\mathcal{H}_k(\pm\Gamma_0)$. From Eq. (32) one can see the dynamics [in the eigenbasis $\{|(+\Gamma_0,k)_\pm\rangle\}$ of the initial Hamiltonian $\mathcal{H}_k(+\Gamma_0)$] can be broken up into steps consisting of successive rotation of the basis by ϕ (corresponding to successive flips of the transverse field) and intermediate accumulation of phases $\mu_{1,2}$ (corresponding to intermediate waitings of duration $T/2$). Clearly if one could adjust the intermediate phases $\mu_{1,2}$ such that their effect is nullified *for all* k, in each cycle, then the system would return very closely to its initial state after every cycle taking any of the eigenstates $\{|(+\Gamma_0,k)_\pm\rangle\}$ as the initial state—the eigenstates of the initial Hamiltonian become Floquet states with degenerate quasienergies (albeit with a different sign, which does not matter in this case). This happens, as explained in the paragraph following Eq. (32), when Γ_0 is large and the condition for maximal freezing [Eq. (24)] is satisfied. For small Γ_0, $\mu_{1,2}$ retain strong k dependence, and hence this massive (k-independent) collapse of the Floquet spectrum will not be possible [see Fig. 1(d)]. It is however worth noting that this simple picture of DMF cannot be extended in cases of continuously driven systems. For example, in the case of sinusoidal driving, the eigenstates of the initial Hamiltonian *do not* tend to return to themselves as one approaches the DMF freezing peak—they retain a strongly k-dependent period of oscillation which actually diverges in the thermodynamic limit for certain modes as the DMF peak is approached. Freezing in that case is visualized as vanishing of the *amplitude of oscillation* of each k mode, rather than "each k-mode coming back to itself." It seems the massive collapse of the entire Floquet spectrum at the maximal DMF is a result of integrability of the model and the simplicity of the driving.

IV. LONG-LIVED SOLITARY OSCILLATION: THE SURVIVOR OF DESTRUCTIVE MANY-BODY INTERFERENCE

Analysis of $M_z(t)$ shows that it is dominated by a distinct solitary oscillation in the long-time limit. The analysis of the response reveals sinusoidal oscillations of only two distinct time scales—one (denoted by ω_0) matches with the driving period T (as expected), while the other, denoted by T_Q (corresponding to frequency $\omega_Q = 2\pi/T_Q$), depends on all the driving parameters. T_Q can be much larger compared to T. Despite the fact that the driving has a large amplitude and high frequency, and the system has several excitable energy levels, we observe only one distinct nontrivial frequency in the response.

This can be understood as follows. The transverse magnetization $M_z(t)$ [Eq. (19)] at time t is a superposition of contributions M_k for all k's [Eq. (25)]. For sufficiently large n, the argument $(2n\omega_k + \delta_k)$ in Eq. (25) will be large (so that its cosine will fluctuate very rapidly with k) while R_k will remain relatively slowly varying. Thus the contributions from neighboring k's will cancel out due to destructive interference (adding up with almost the same amplitude but rapidly varying phase) over any small intervals of k, except those around the stationary points of ω_k (with respect to k). In the neighborhood of its stationary points, ω_k is expected to vary slowly with k, and hence the contributions from different k's within such a neighborhood are expected to add up constructively. Elsewhere the contributions adds up destructively and can hence be ignored. Thus we may write

$$\int_0^\pi R_k \cos(2n\omega_k + \delta_k)dk \approx R_{\pi/2} \int_{\frac{\pi}{2}-\epsilon}^{\frac{\pi}{2}+\epsilon} \cos(2n\omega_k + \delta_{\pi/2})dk. \quad (32)$$

By Taylor expansion of ω_k about the stationary point, we can write

$$\cos(2n\omega_k + \delta_{\pi/2}) = \cos(2n\omega_{\pi/2} + \delta_{\pi/2}) \cos\left(nC\left[k - \frac{\pi}{2}\right]^2\right), \quad (33)$$

where $C = (d^2\omega_k/dk^2)_{k=\pi/2}$. This finally gives

$$M_z(n) \approx M_0 + \frac{a}{\sqrt{n}} \cos(n\omega_Q + \delta_{\pi/2}), \quad (34)$$

where

$$\omega_Q = 2\omega_{\pi/2} = 2\cos^{-1}\{1 - \cos^2\phi[1 - \cos(\mu_1 + \mu_2)]\} \quad (35)$$

and

$$M_0 = -1 + \frac{2}{\pi}\int_0^\pi A_k\, dk, \quad a = R_{\pi/2}\sqrt{\frac{\pi}{2C}}.$$

The above arguments are quite generic, and variants of them can be found in other contexts (see, e.g., Ref. 24). The survival of a few such distinct oscillations of very long (compared to the driving period) time scales has also been observed in an infinite-range transverse Ising model driven periodically in time.[25] The results described in this section are a manifestation of more general results regarding periodically driven quantum many-body systems (Ref. 26).

We see from Eq. (35), when the freezing condition ($p =$ integer) is satisfied, ω_Q vanishes for large Γ_0 up to terms linear in $1/\Gamma_0$ and $a \to 0$ and $M_0 \to 1$. The numerical calculation of M_z [using Eqs. (17)–(20)] is presented in Fig. 2. The discrete Fourier transform of $M_z(t)$ also shows two peaks corresponding to ω_0 and ω_Q. The value of ω_Q obtained from there matches pretty well with the analytical expression in Eq. (35).

Though our results are demonstrated for rectangular pulses, a similar argument can be extended for other forms of periodic drivings. The only requirements for the appearance of solitary oscillations (if they exist) are certain analytical properties of the response, continuity of the spectrum, and long driving time. Hence such oscillations are expected to appear quite generically in many periodically driven coherent many-body quantum systems, but analytical results might not be easy to extract in all cases. An extension of DMF for some other forms of periodic drivings may be achieved following Ref. 27.

The phenomena we discuss above are the result of quantum coherence. Further investigations in this direction are likely to reveal many new phenomena (see, e.g. Ref. 28). A natural open question is whether they are realizable in real experiments, in the presence of the inevitable experimental imperfections existing within the present-day setups. Such experimental realizations would also allow for exploring these phenomena in more generic nonintegrable systems where accurate theoretical investigations could be difficult. Experimental observation of the above phenomena might be possible within the framework of coherent quantum simulation using trapped ions and atoms in optical lattice. In particular, DMF will have a clear signature even for very small systems consisting of few spins realized in the experimental systems above, since at the freezing peaks *all* the momentum modes freeze independent of system size, whereas away from the peaks considerable dynamics is expected for any system size. Coherent simulation of a transverse Ising Hamiltonian with a time-dependent transverse field, which can be varied adiabatically, has also been realized experimentally. In layered linear Paul traps using $^{171}Yb^+$ ions[11] and $^{25}Mg^+$ ions,[12] they realized a transverse field Ising model where they could tune both spin-spin interactions and the transverse field with time.

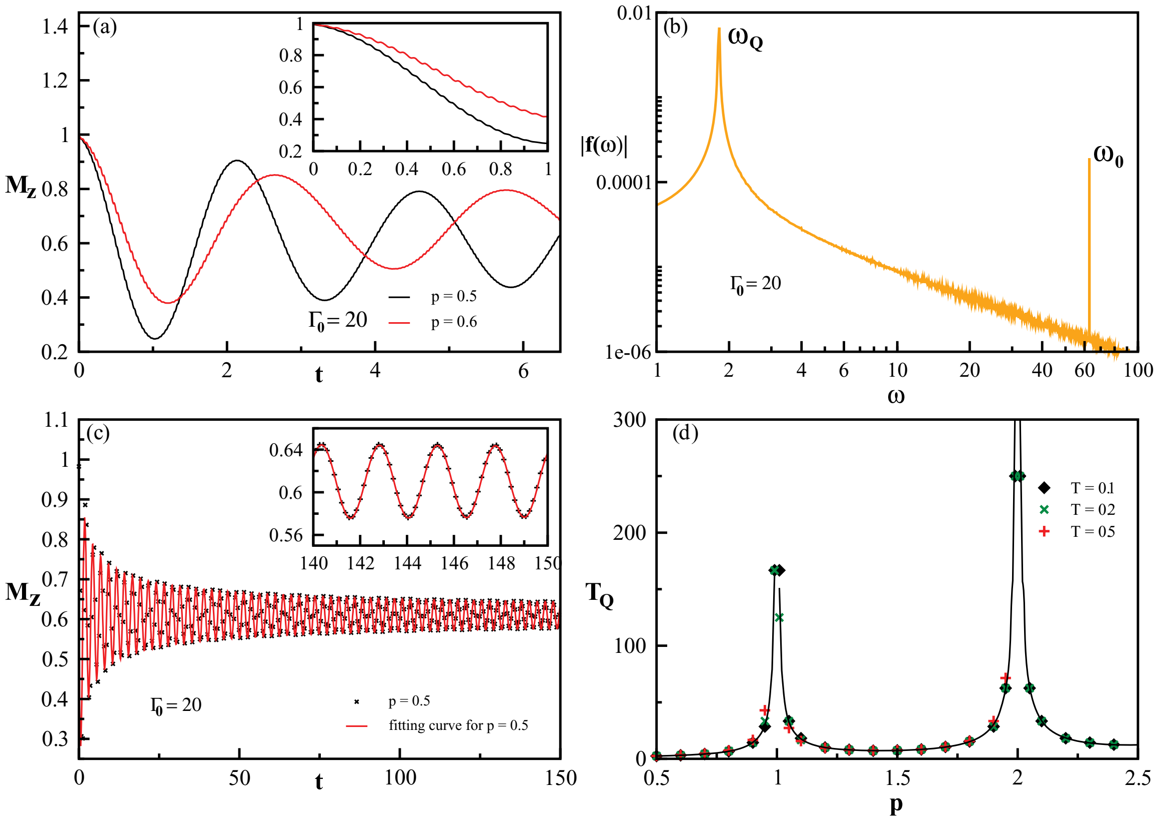

FIG. 2. (Color online) Features of magnetization obtained by numerical integration of Eqs. (25) and (19). (a) Oscillations of two distinct time scales are observed in $M_z(t)$. In addition to the expected one with period T (matching to the driving), there is an additional longer time scale prominently visible. (b) Fourier transform of $M_z(t)$ showing two time scales visible in frame (a): two distinct peaks at angular frequencies ω_Q and ω_0 are observed. The peak at $\omega_Q = 1.822$ in the figure matches quite well with the estimation (1.815) from Eq. (35), while $\omega_0 \approx 2\pi/T$, where $T = 0.1$ is the driving period. (c) Long-time behavior of $M_z(t)$ obtained numerically (points) and that given by fitting Eq. (34) (continuous curve) is shown. The envelop corresponding to the $1/\sqrt{n}$ decay (Eq. (34)) is visible. (d) Variation of $T_Q = 2\pi/\omega_Q$ with p for $T = 0.1$ obtained by Fourier transform. T_Q tends to blow up (i.e., ω_Q vanishing up to order $1/\Gamma_0$) at integer values p—consistent with the observed maximal freezing at integer p. The points correspond to the values obtained from Fourier transform and the continuous line is obtained from Eq. (35) ($\hbar = 1$).

V. SUMMARY

We investigate the dynamics of the transverse Ising chain under periodic instantaneous quenches of the transverse field. We make two interesting observations.

(i) In the high amplitude ($\Gamma_0 \gg J$) and fast quenching ($T \ll J$) limits we observe DMF—we see that the driven system freezes close to its initial state and the degree of freezing is a highly *nonmonotonic* function of the pulse amplitude Γ_0 and period T. The extremal freezing is observed for $\Gamma_0 T/\hbar = n\pi$ ($n =$ positive integers). At these freezing "peaks," the system remains frozen very strongly *independent* of its initial state. This freezing drastically contrasts the classical notion of monotonic (with respect to the driving rate) freezing of a system under fast periodic driving—a faster driving would give it less time to react and hence would leave it more frozen. Quantum simulation of the transverse Ising chain has already been realized experimentally—the phenomena should be amenable to experimental verification within the said setup and similar others for quantum simulation.

(ii) In the response dynamics, we observe the emergence of a *single, distinct* time scale, T_Q (in addition to the time scale of the driving), in the long-time limit. This distinct oscillation decays much slower than other oscillations, following a $1/\sqrt{n}$ ($n =$ number of sweeps) envelop. Dominance of a single nontrivial frequency in the response is surprising, since the system is driven with pulses with high (compared to the intrinsic energy scale given by the spin-spin interaction J) amplitude and frequency. We show that this surviving time scale represents oscillations of the nonlocal momentum modes lying within a neighborhood of a unique point in the momentum space ($k = \pi/2$ here), where the contributions from the neighboring modes add up constructively. For all other parts of the momentum space such interferences are destructive, leading to mutual cancellation of oscillations of the neighboring modes.

ACKNOWLEDGMENTS

The authors are grateful to Andre Eckardt, Joseph Samuel, and Supurna Sinha for valuable comments. A.D. acknowledges the support of the US Department of Energy through the LANL/LDRD Program. S.D. acknowledges financial support from CSIR (India).

*Corresponding author: arnabdas@pks.mpg.de

[1] A. Polkovnikov, K. Sengupta, A. Silva, and M. Vengalattore, Rev. Mod. Phys. **83**, 863 (2011); J. Dziarmaga, Adv. Phys. **59**, 1063 (2010).

[2] A. Chandra, A. Das, and B. K. Chakrabarti, *Quantum Quenching, Annealing and Computation*, Lecture Notes in Physics Vol. 802, (Springer, New York, 2010).

[3] W. H. Zurek, U. Dorner, and P. Zoller, Phys. Rev. Lett. **95**, 105701 (2005); B. Damski, *ibid*. **95**, 035701 (2005); J. Dziarmaga, *ibid*. **95**, 245701 (2005).

[4] T. W. B. Kibble, J. Phys. A **9**, 1387 (1976); W. H. Zurek, Nature (London) **317**, 505 (1985).

[5] A. Das, Phys. Rev. B **82**, 172402 (2010).

[6] A. Eckardt, C. Weiss, and M. Holthaus, Phys. Rev. Lett. **95**, 260404 (2005).

[7] A. Eckardt and M. Holthaus, Europhys. Lett. **80**, 50004 (2007).

[8] M. Lewenstein *et al*., Adv. Phys. **56**, 243 (2007).

[9] I. Buluta and F. Nori, Science **326**, 108 (2009).

[10] B. Kraus, Phys. Rev. Lett. **107**, 250503 (2011).

[11] K. Kim *et al*., New J. Phys. **13**, 105003 (2011); Nature (London) **465**, 590 (2010).

[12] A. Friendenauer *et al*., Nat. Phys. **4**, 757 (2008).

[13] B. K. Chakrabarti, A. Dutta, and P. Sen, *Quantum Ising Phases and Transitions in Transverse Ising Models* (Springer-Verlag, Heidelberg, 1996); S. Sachdev, *Quantum Phase Transition* (Cambridge University Press, Cambridge, UK, 2001); S. Dattagupta, *Paradigm Called Magnetism* (World Scientific, Singapore, 2008).

[14] A. Eckardt and M. Holthaus, Phys. Rev. Lett. **101**, 245302 (2008); F. Pellegrini, C. Negri, F. Pistolesi, N. Manini, G. E. Santoro, and E. Tosatti, *ibid*. **107**, 060401 (2011); S. Miyashita, H. De Raedt, and B. Barbara, Phys. Rev. B **79**, 104422 (2009); M. G. Bason *et al*., Nat. Phys. **8**, 147 (2012).

[15] D. H. Dunlap and V. M. Kenkre, Phys. Rev. B **34**, 3625 (1986).

[16] F. Grossmann, T. Dittrich, P. Jung, and P. Hänggi, Phys. Rev. Lett. **67**, 516 (1991).

[17] M. Grifoni and P. Hänggi, Phys. Rep. **304**, 229 (1998).

[18] A. Eckardt, M. Holthaus, H. Lignier, A. Zenesini, D. Ciampini, O. Morsch, and E. Arimondo, Phys. Rev. A **79**, 013611 (2009).

[19] E. Arimondo *et al*., Adv. Atomic Mol. Phys. (in press), arXiv:1203.1259.

[20] E. Lieb, T. Schultz, and D. Mattis, Ann. Phys. (NY) **16**, 407 (1961).

[21] A. Mostafazadeh, J. Phys A **31**, 9975 (1998).

[22] A. Eckardt and M. Holthaus, J. Phys.: Conf. Ser. **99**, 012007 (2008).

[23] S. Mondal, D. Pekker, and K. Sengupta, arXiv:1204.6331v2.

[24] Y. Pomeau and P. Resibois, Phys. Rep. **19**, 63 (1975).

[25] A. Das, K. Sengupta, D. Sen, and B. K. Chakrabarti, Phys. Rev. B **74**, 144423 (2006).

[26] A. Das (unpublished).

[27] A. Sacchetti, J. Phys. A **34**, 10293 (2001).

[28] A. Das and R. Moessner, arXiv:1208.0217v1 (2012).